TEEC and azimuthal correlations in forward γ -hadron production in proton-proton and proton-lead collisions at LHC

Ishita Ganguli^a, Piotr Kotko^a

^a AGH University Of Krakow, Faculty of Physics and Applied Computer Science, al. Mickiewicza 30, 30-059 Kraków, Poland

Abstract

We investigate photon-hadron Transverse Energy-Energy Correlation (TEEC) and azimuthal correlations in the forward rapidity region for proton-proton and proton-lead collisions within the small x saturation formalism based on the Color Glass Condensate (CGC), supplemented by the initial-state and final-state parton shower simulation and hadronization using CASCADE. The study was performed in light of the upcoming FoCal detector of ALICE and the ATLAS detector upgrades with the extended pseudorapidity coverage. We predict a significant difference, at hadron-level, between the normalized TEECs in proton-proton and proton-lead collisions. Having a direct access to partonic subprocesses we also directly investigate the impact of the parton shower and hadronization on the TEEC. The ordinary azimuthal γ -hadron correlations show substantial suppression for proton-lead collision, as predicted earlier at parton-level.

1 Introduction

Event shape observables, such as thrust, have long been used in precision studies in Quantum Chromodynamics (QCD), see eg. [1–3]. They are defined to be infrared and collinear safe, meaning they are designed to be robust against soft gluon emissions and collinear splittings. By quantifying complex multi-particle final states with the use of simple scalar quantities, event shape variables allow for precise comparisons between experimental measurements and perturbative QCD calculations. Event shape observables in e^+e^- collisions have been studied up to next-to-next-to-leading order at fixed order [4-6], and at next-to-next-to-leading logarithm [7-9]. Energy-Energy correlators (EEC), first introduced in [10,11], are more differential variants of the C-parameter event shape variable and measure the correlations of energy flow along directions on celestial sphere see e.g., [12-14] for experimental determination and [15, 16] for more comprehensive reviews and summary of recent computations. Here, let us mention, that despite relative simplicity of the observable, the full analytical result at NLO level in QCD was computed not that long ago [17]. In parallel, EEC are interesting observables to apply holography to study their non-perturbative aspects [18] (see also [16] and references therein). Transverse Energy-Energy Correlators (TEEC) [19] are a natural extension of the EEC for hadron colliders. TEEC, by definition, suppresses contributions from small transverse energy hadrons. Final states in TEEC can be jets or hadrons. In the latter case, it gives quite a direct access to underlying hard partonic process, due to the suppression of soft radiation (see e.g. [20] in the context of DIS). Jet TEEC was measured at LHC in the context of strong coupling studies [21,22]. However, in general, sound jet reconstruction requires significant p_T , which is an unwanted feature in gluon saturation searches that should occur at small $x \sim p_T/\sqrt{s}$. Therefore, in the following work we shall focus on TEEC defined for hadrons.

The process we are looking into is the forward production of photons and hadrons,

$$p(P_A) + A(P_B) \rightarrow \gamma(p_\gamma) + h(p_h),$$
 (1)

where A is either a proton or a lead nucleus. At perturbative level, a single colored state makes this observable a favorable starting point for gluon saturation studies in the near-future high luminosity LHC forward calorimeters [23]. Gluon saturation phenomenon was predicted in QCD long time ago [24,25] (see also the book [26]), and later developed mainly through the Color Glass Condensate (CGC) effective theory (see e.g. [27] for a review). Although a direct observation of gluon saturation remains challenging, several experimental signatures serve as indirect evidence [28–30]; still, there are other mechanisms that can potentially be at play, such as the so-called leading twist nuclear shadowing [31] or parton energy loss. Discriminating between different mechanisms requires a selection of observables and broad range of kinematics. The computations of scattering processes in CGC are incomparably more involved than in collinear factorization. There are a multitude of reasons for that, in particular, the CGC computations include multiple interactions and thus higher twist corrections. Production of photons has been computed in CGC at LO in [32,33] with many follow-up computations for proton-proton and proton-nucleus collisions [34–42] as well as electron-nucleus collisions [43–45].

The purpose of this work is to compute both TEEC and photon-hadron azimuthal correlations, in the kinematics of the near-future ALICE and ATLAS upgrades. FoCal, or Forward Calorimeter [46] is a part of the ALICE detector in LHC and is planned to cover a very forward pseudorapidity window: $3.8 < \eta < 5.1$. On the other hand, the ATLAS calorimeter is proposed to have an increased pseudorapidity coverage of $|\eta|$ up to 4 [47]. The distinctive feature of our computation is inclusion of the full parton shower and hadronization, on top of the CGC setup (in the form of the hybrid k_T -factorization that convolutes the dipole TMD gluon distribution with kinematic constraints and DGLAP correction with off-shell gauge invariant leading order amplitude). The work is a significant extension of [48] and provides a parallel study to [49] from the Monte Carlo perspective.

The γ -hadron TEEC in proton-proton or proton-nucleus collision has been defined [50]:

$$\frac{d\Sigma}{d\phi} = \sum_{h} \int d\sigma \frac{E_{T\gamma} E_{Th}}{E_{T\gamma} \sum_{h'} E_{Th'}} \delta(\phi_{\gamma h} - \phi)$$
 (2)

where E_T is the transverse energy and $\phi_{\gamma h}$ is the azimuthal angle between the leading photon and each hadron, the sum being over all hadrons.

The photon can either be a direct product of the hard interaction, or can be created later during the shower. Such a hadron-level computation has many challenges. At present there is no general purpose event generator that does the parton-level computation with CGC framework, followed by the parton showers and hadronization. Although there are generators that include small-x effects or Pomeron self-interactions (see e.g. [51–58]), in our computation we would like to adhere to TMD-like factorization based on the CGC framework. While the leading order partonic cross section is straightforward to compute using e.g. KATIE Monte Carlo [59], there does not exist a Monte Carlo generator that can perform a shower with gluon recombination, consistent with the Balitsky-Kovchegov (BK) nonlinear evolution equation [60, 61] for TMD gluon distribution, not mentioning the full B-JIMWLK equation [60, 62–67]. There is however the CASCADE Monte Carlo [68], which is capable of turning the information contained in the TMD gluon distribution into a cascade of partons (see also [69]). Such an approach has already been implemented in the past, see [70,71].

As mentioned before, γ -hadron and γ -jet correlations will be an important part of the future forward physics program at LHC. γ -hadron correlations in proton-proton and proton-lead collisions have been measured by ALICE [72,73], but with different goals in mind. Although some of these studies do indicate the presence of initial state effects, most of these measurements were performed in lower rapidities. On the other hand, γ -jet correlations have been studied by ATLAS [74,75] in proton-proton collisions in the past.

2 Results

In this section, we provide numerical results for TEEC and azimuthal correlations for γ -hadron production in proton-proton (pp) and proton-lead (pPb) collisions within the FoCal detector acceptance as part of future ALICE upgrade and the extended ATLAS kinematics. Below, we describe

first the theoretical framework and the tools used to perform the numerical computations. Next, we will describe in details the kinematic cuts we impose and discuss the results.

The computation is a two-stage process. We first generate the Monte Carlo samples for the partonic processes $q(\bar{q})g^* \to q(\bar{q})\gamma$, where g^* represents an off-shell gluon, that, in addition to the transverse momentum, carries only longitudinal momentum parallel to the mother hadron (nucleus), but no longitudinal momentum of the other hadron. Such an approximation is dictated by the high energy limit in the spirit of the high energy factorization [76,77] (actually the hybrid factorization [78, 79]), which is also consistent with the CGC approach [80], up to the definition of the gluon distribution. We shall not repeat here the factorization formulae – see e.g. [48] for details. The partonic Monte Carlo samples were generated in KATIE [59] that implements the high energy factorization and provides an efficient way of computing off-shell gauge invariant amplitudes [81,82]. The collinear PDF describing the dilute projectile was set to CT18NLO and provided via LHAPDF [83]. The small-x dipole TMD gluon distribution was taken to be the Kutak-Sapeta (KS) fit to HERA data [84]. This choice is dictated by the fact that its nonlinear evolution is based on the unified BK/DGLAP framework developed by Kwieciński and collaborators [85,86], which includes, in particular, the kinematic constraint. The output from KATIE are Les Houches (LHE) files which can then be processed by other Monte Carlo generators. The second stage of the computation is to perform the parton shower and hadronization. As described in the *Introduction*, we use the CASCADE Monte Carlo [68], which we run with the nonlinear TMD gluon distribution (with full awareness of the limitations of such a procedure). After performing the final-state and initial-state shower, taking into account the explicit transverse momentum of the off-shell gluons, CASCADE does the full hadronization utilizing routines from PYTHIA.

For the FoCal kinematics the parton-level events were generated at a center-of-mass energy of 8.8 TeV per nucleon in KATIE, for both pp and pPb. The colored partons were produced within an extended pseudorapidity window of $2.8 < \eta < 6.1$ and the direct photons with $3.8 < \eta < 5.1$. We further imposed a minimum transverse momentum condition of 7 GeV on both the parton and the direct photon (we discuss the sensitivity of this choice later in this section). For ATLAS kinematics the center-of-mass energy was set to 8.16 TeV per nucleon and the parton and the direct photon were required to have a minimum transverse momentum of 5 GeV. Here, the partons were produced within the extended pseudorapidity $1.7 < \eta < 5.0$, and the direct photons with $2.7 < \eta < 4.0$. Although the ATLAS detector covers both hemispheres, we only focus on the forward region for the purpose of this study. For both kinematical setups we require that the minimum distance R between the final states in the $\eta - \phi$ plane is > 0.1. At parton level, the factorization and renormalization scales were set to the average p_T of the final states. As mentioned above, the partons were generated within a slightly broader pseudorapidity window, as compared to the constraints applied on the hadrons. This is to account for hadrons produced within the detector acceptance but produced from partons emitted outside this range.

To construct the final observables we collect the photons and charged hadrons with $2.7 < \eta < 4.0$ for the ATLAS kinematics and with $3.8 < \eta < 5.1$ for FoCal. The photons were required to have a minimum transverse momentum of 5 GeV in both cases. No such transverse momentum constraints were imposed on the hadrons. However, we only choose the events where at least one hadron possesses transverse momentum above a $p_{T\,\mathrm{Trig}}$. We study the impact of this $p_{T\,\mathrm{Trig}}$ later in this section.

Fig. 1 shows γ -hadron TEEC in pp and pPb for both ATLAS (left) and FoCal (right) kinematics. There is a significant suppression in pPb TEEC compared to pp. The suppression is more pronounced in the back-to-back ($\phi \sim \pi$) region. Notice, our TEEC definition involves a normalization factor, so the suppression is due to an interplay of the shape of the TMD distributions for proton and lead, and not just the overall suppression of the lead TMD. In these computations the $p_{T\,\mathrm{Trig}}$ was set to 5 GeV. In order to better visualize this suppression, in Fig. 2 we show the factor $R_{\mathrm{pPb}}^{\mathrm{TEEC}}$ defined as:

$$R_{\mathrm{p}Pb}^{\mathrm{TEEC}} = \frac{\left(\frac{1}{\Sigma} \frac{d\Sigma}{d\phi}\right)_{\mathrm{p}Pb}}{\left(\frac{1}{\Sigma} \frac{d\Sigma}{d\phi}\right)_{\mathrm{pp}}}.$$

Although for a wide range of ϕ it is close to 1, there is a sharp drop near the back-to-back region. We show $R_{\rm pPb}^{\rm TEEC}$ for two different $p_{T\,\rm Trig}$ values, 5 GeV and 10 GeV. For a $p_{T\,\rm Trig}$ of 10 GeV (in blue), we see a suppression of about $\sim 20\%$ for ATLAS kinematics (left) and about $\sim 22\%$ for

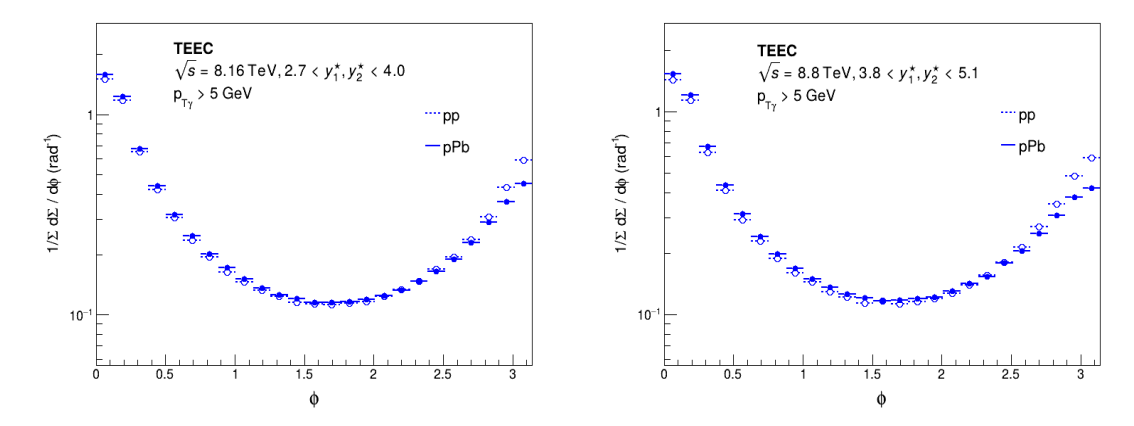


Figure 1: Normalized γ -hadron TEEC in pp and pPb collisions at CM energy 8.16 TeV, 2.7 $< y_1^*, y_2^* < 4.0$ (on the left) and at CM energy 8.8 TeV, $3.8 < y_1^*, y_2^* < 5.1$ (on the right). The photon in both cases was required to have a minimum transverse momentum of 5 GeV. Although there was no such restriction on the hadron transverse momentum, the events were required to have at least one hadron with $p_T > 5$ GeV.

FoCal near $\phi \sim \pi$. For $p_{T\,\mathrm{Trig}} = 5$ GeV (in red), we see a stronger suppression of about $\sim 24\%$ for ATLAS (left) and about $\sim 30\%$ for FoCal kinematics near $\phi \sim \pi$. This shows how the shape of the distribution varies with the $p_{T\,\mathrm{Trig}}$.

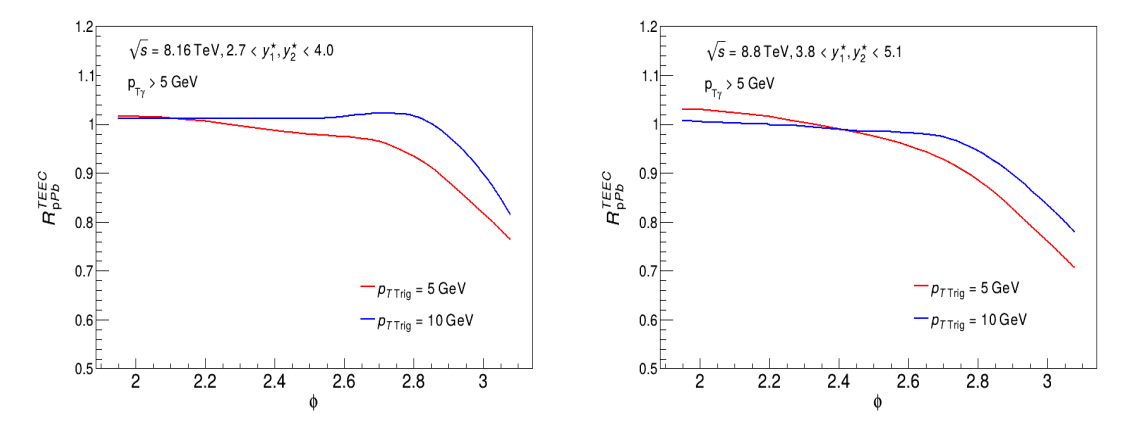


Figure 2: $R_{\rm pPb}^{\rm TEEC}$ for γ -hadron production in pp and pPb collisions at CM energy 8.16 TeV, $2.7 < y_1^*, y_2^* < 4.0$ (on the left) and at CM energy 8.8 TeV, $3.8 < y_1^*, y_2^* < 5.1$ (on the right). The photon in both cases was required to have a minimum transverse momentum of 5 GeV. Although there was no such restriction on the hadron transverse momentum, the events were required to have at least one hadron with $p_T > 5$ GeV (in red) and $p_T > 10$ GeV (in blue).

In Fig. 3, we show the azimuthal correlation (defined as the differential cross section in the azimuthal angle) of the leading photon-hadron pair within the ATLAS (left) and FoCal (right) kinematics. $p_{T\,\mathrm{Trig}}$ was taken to be 5 GeV. Similar to the TEEC distributions, we observe a significant suppression in pPb differential cross-section compared to pp, which is much stronger in the back-to-back region, consistent with the CGC picture. The results in the FoCal kinematics correspond to a stronger suppression. Here the suppression is a direct effect of the suppression of the maximum of the TMD gluon distribution for lead at small-x. We note, that the suppression is still visible, after the hadronization and shower. The usual nuclear modification factor R_{pPb}

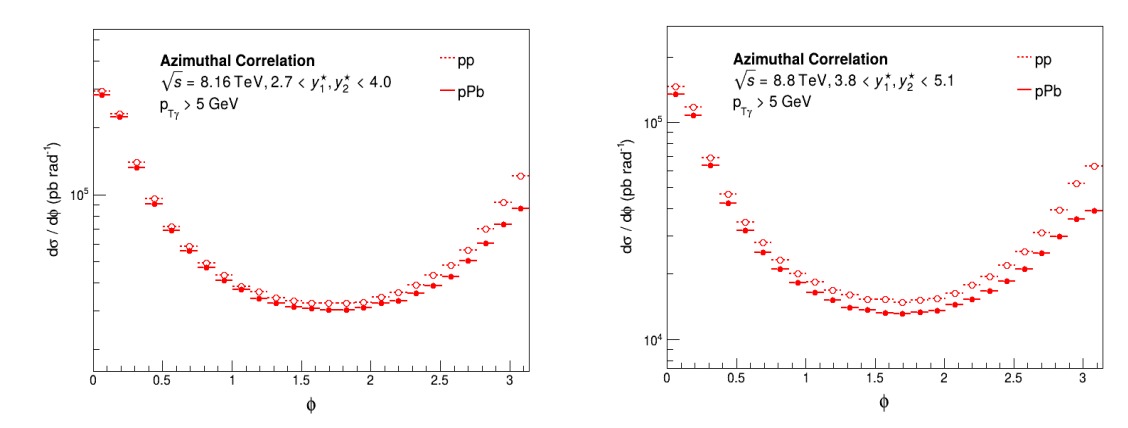


Figure 3: Leading γ -hadron azimuthal correlation in pp and pPb collisions at CM energy 8.16 TeV, $2.7 < y_1^*, y_2^* < 4.0$ (on the left) and at CM energy 8.8 TeV, $3.8 < y_1^*, y_2^* < 5.1$ (on the right). The photon in both cases was required to have a minimum transverse momentum of 5 GeV. Although there was no such restriction on the hadron transverse momentum, the events were required to have at least one hadron with $p_T > 5$ GeV.

defined as:

$$R_{pPb} = \frac{1}{A} \frac{\left(\frac{d\sigma}{d\phi}\right)_{pPb}}{\left(\frac{d\sigma}{d\phi}\right)_{pp}},$$

is shown in Fig. 4. Here too, we show the nuclear modification factor for two different $p_{T\,\mathrm{Trig}}$ values of 5 and 10 GeV. $R_{\mathrm{p}Pb}$ is close to but smaller than one in the shown ϕ range and exhibits a stronger suppression for both $p_{T\,\mathrm{Trig}}$ values in comparison to the TEEC ratio, especially in the back-to-back region. The factor drops by $\sim 30\%$ for $p_{T\,\mathrm{Trig}}$ 5 GeV (in red) for ATLAS (left) and close to $\sim 40\%$ for FoCal (right) kinematics. Similarly for $p_{T\,\mathrm{Trig}} = 10$ GeV, there's a stronger suppression of $\sim 30\%$ observed in FoCal, as compared to $\sim 25\%$ in ATLAS.

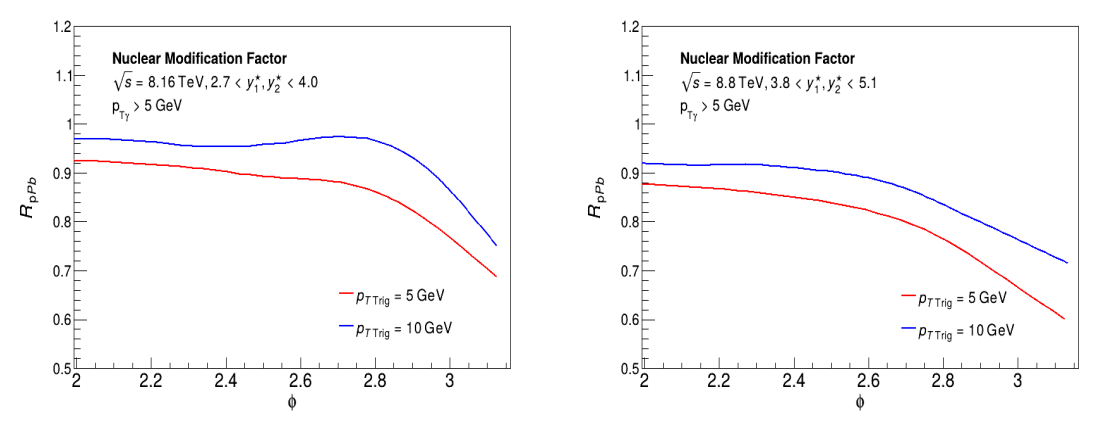


Figure 4: Nuclear modification factor for γ -hadron production in pp and pPb collisions at CM energy 8.16 TeV, $2.7 < y_1^*, y_2^* < 4.0$ (on the left) and at CM energy 8.8 TeV, $3.8 < y_1^*, y_2^* < 5.1$ (on the right). The photon in both cases was required to have a minimum transverse momentum of 5 GeV. Although there was no such restriction on the hadron transverse momentum, the events were required to have at least one hadron with $p_T > 5$ GeV (in red) and $p_T > 10$ GeV (in blue).

In our study, we defined the azimuthal correlation observable for the lading photon and the leading hadron. Alternatively, we could have defined this observable for the leading photon and any hadron with the presence of a trigger hadron in both cases. Let us therefore discuss how these hadron-level observables compare with each other and with TEEC. Fig. 5 shows TEEC

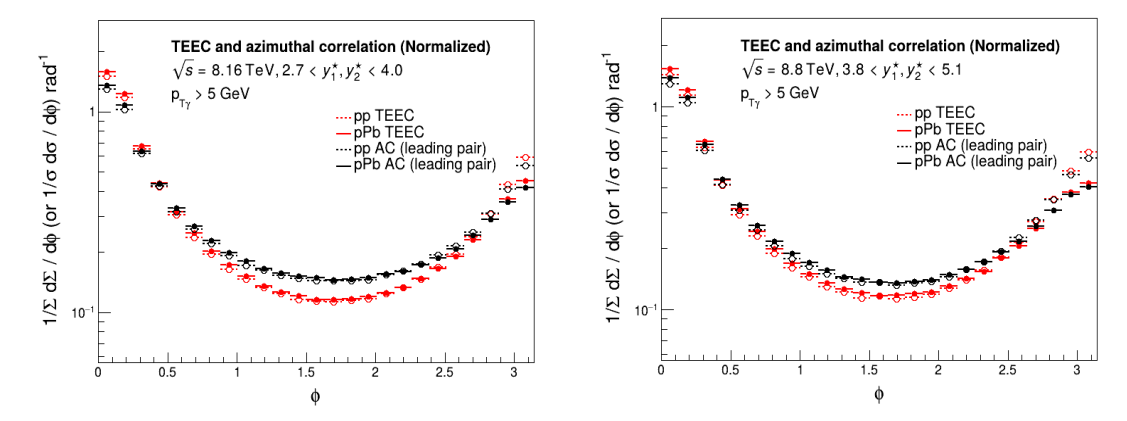


Figure 5: Comparison of normalized TEEC and azimuthal correlation of the hardest γ -hadron pair in pp and pPb collisions at CM Energy 8.16 TeV, $2.7 < y_1^*, y_2^* < 4.0$ (left) and at CM energy 8.8 TeV, $3.8 < y_1^*, y_2^* < 5.1$ (right). The photon in both cases was required to have a minimum transverse momentum of 5 GeV. Although there was no such restriction on the hadron transverse momentum, the events were required to have at least one hadron with $p_T > 5$ GeV.

and azimuthal correlation of the leading photon-hadron pair and Fig. 6 on the other hand is the azimuthal correlation of the leading photon with a randomly chosen hadron. The azimuthal correlation distributions have been normalized for comparison purposes. Although the overall shape is quite similar, the normalized azimuthal correlations are generally flatter, especially the one defined for leading-photon-any-hadron. This picture is consistent with our expectations from perturbative QCD.

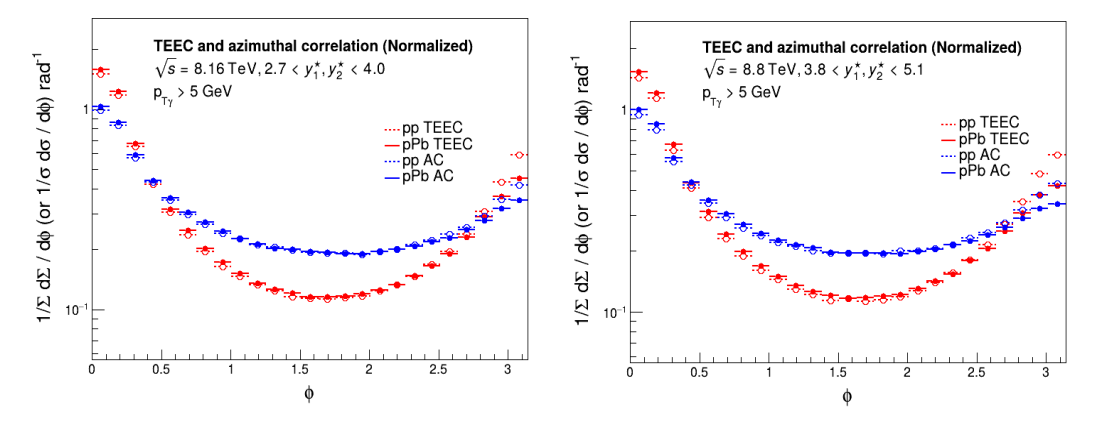


Figure 6: Comparison of normalized TEEC and azimuthal correlation of the hardest γ and a randomly chosen hadron in pp and pPb collisions at CM Energy 8.16 TeV, $2.7 < y_1^*, y_2^* < 4.0$ (left) and at CM energy 8.8 TeV, $3.8 < y_1^*, y_2^* < 5.1$ (right). The photon in both cases was required to have a minimum transverse momentum of 5 GeV. Although there was no such restriction on the hadron transverse momentum, the events were required to have at least one hadron with $p_T > 5$ GeV.

ATEEC or the asymmetry of TEEC is defined as the difference:

$$\mathbf{ATEEC} = \frac{1}{\Sigma} \frac{d\Sigma}{d\tau} |_{\tau} - \frac{1}{\Sigma} \frac{d\Sigma}{d\tau} |_{1-\tau} , \qquad (3)$$

where $\tau = \frac{1+\cos\phi}{2}$. ATEEC has been found to be quite useful in analyzing the shape of TEEC distributions and in practice has been used alongside TEEC. Fig. 7 shows this asymmetry for

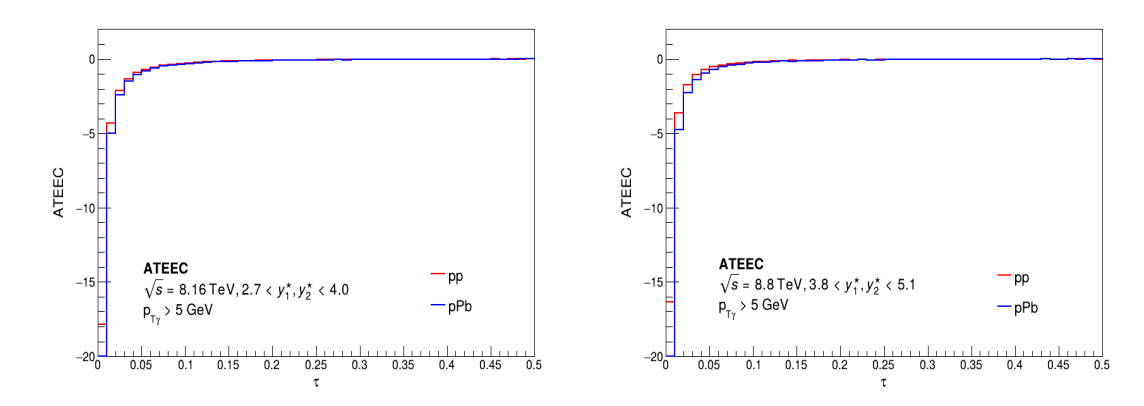


Figure 7: Asymmetry in γ -hadron TEEC (ATEEC) in pp and pPb collisions at CM energy 8.16 TeV, $2.7 < y_1^*, y_2^* < 4.0$ (on the left) and at CM energy 8.8 TeV, $3.8 < y_1^*, y_2^* < 5.1$ (on the right). The photon in both cases was required to have a minimum transverse momentum of 5 GeV. Although there was no such restriction on the hadron transverse momentum, the events were required to have at least one hadron with $p_T > 5$ GeV.

ATLAS (left) and FoCal (right) kinematics. The quantity is negative throughout. It is highly asymmetric for both pp and pPb in the low τ ($\tau \sim 0$) region, which corresponds to the backto-back limit. It appears that pPb TEEC is more asymmetric than pp, although both sets of distributions become more symmetric towards $\tau \sim 0.5$ or $\phi \sim \pi/2$.

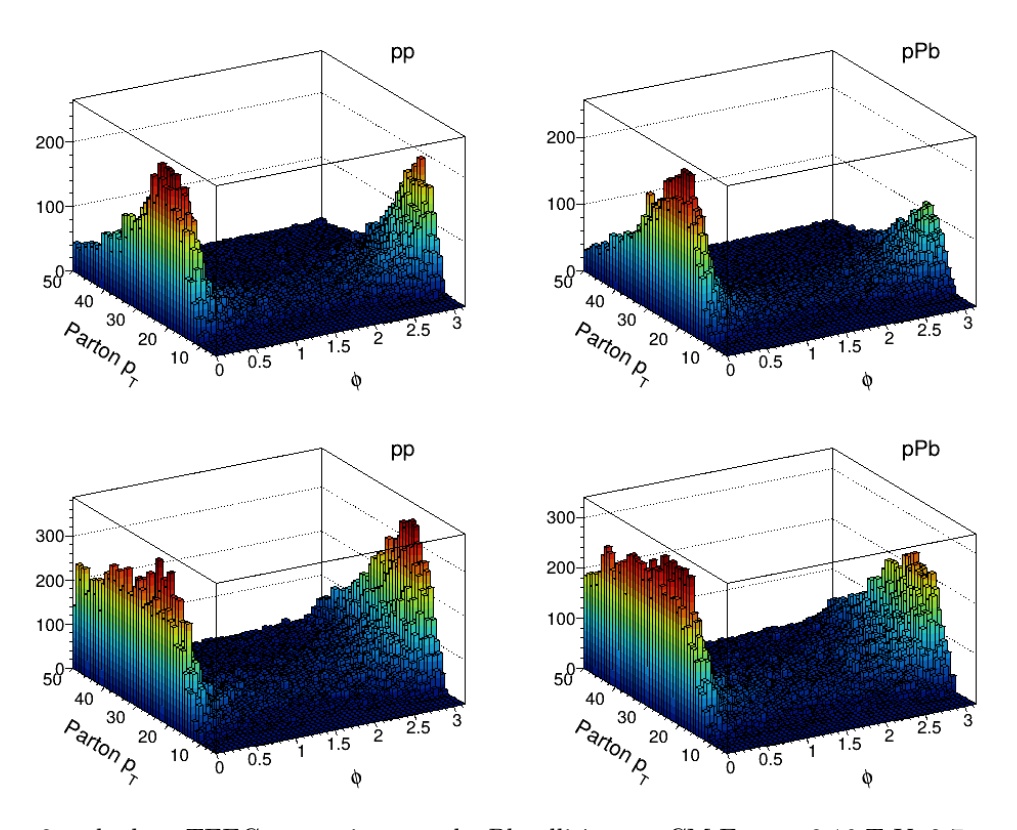


Figure 8: γ -hadron TEEC counts in pp and pPb collisions at CM Energy 8.16 TeV, $2.7 < y_1^*, y_2^* < 4.0$ (bottom row) and CM energy 8.8 TeV, $3.8 < y_1^*, y_2^* < 5.1$ (top row) w.r.t. their azimuthal separation (ϕ) and the p_T of hardest parton. The vertical axis here reflects event counts, and not the TEEC defined above.

Let us finally see how much does the earlier assumption about the minimum parton transverse momentum impact the final observable. Here, we mean the cut imposed in KATIE at the parton-level of the computation. Fig. 8 shows a 2D histogram, where the z-axis represents event counts with respect to the azimuthal angle between the leading photon and each hadron accounted, with the corresponding p_T of the leading parton (in the partonic subprocess). For this objective, the trigger was set to 10 GeV. As seen from the plots, the cuts imposed on hadrons are sufficient to induce the proper parton-level kinematics. In particular, there is very little contribution from events with partons having p_T smaller than the trigger. Finally, Fig. 9 shows the comparison of

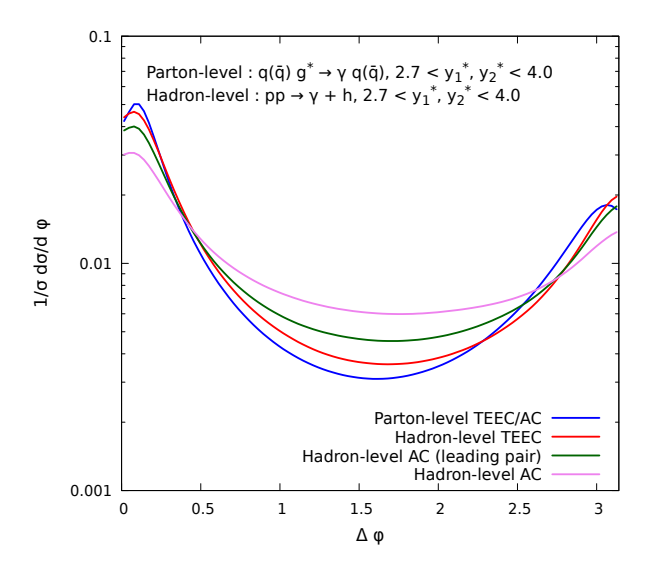


Figure 9: Comparison of parton level azimuthal correlation from KATIE, with γ -hadron TEEC and azimuthal correlation as obtained post hadronization via CASCADE in pp collisions at CM energy 8.16 TeV, with $2.7 < y_1^*, y_2^* < 4.0$ (all normalized). The partons were generated with a minimum transverse momentum of 5 GeV in KATIE.

these observables with the parton-level azimuthal correlations (we plot this only for $pp \to \gamma + h$ in ATLAS kinematics for brevity). More precisely, we compare the parton-level correlation with the hadron-level TEEC (red) and azimuthal correlation of both the leading pair (in green) and leading photon with a randomly chosen hadron (in pink). Obviously, at parton-level the TEEC is identical with azimuthal correlation between the direct photon and the parton; both the direct photon and parton were required to have a minimum transverse momentum of 5 GeV and were generated within $2.7 < \eta < 4.0$ in KATIE. The hadron-level TEEC and azimuthal correlations were computed as explained earlier. As expected, the parton-level correlations (or TEEC) are very peaked in the collinear and back-to-back regions. The TEEC, despite being a hadron-level observable, follows the parton dynamics quite closely.

3 Summary

In this work, we present detailed numerical results for forward γ -hadron TEEC and azimuthal correlations in both proton-proton (pp) and proton-lead (pPb) collisions within the kinematics of the near-future ALICE and ATLAS upgrades. We used the CGC-based formalism in the form of hybrid k_T factorization, with the TMD gluon distribution encoding the gluon saturation effects at small-x. We used a two-stage procedure to obtain the hadron-level results. The parton-level computation was done using the KATIE Monte Carlo, while the hadronization and parton shower was performed using CASCADE. It is worth mentioning at this point, that although this computation incorporates the nonlinear gluon dynamics, there is no explicit parton-recombination implemented in the CASCADE. On the other hand, the rate of parton production in the shower is correctly taken into account. We therefore claim that such a computation captures the most important features.

We observe a significant suppression of both the normalized TEEC and azimuthal correlations in pPb compared to pp. In the former, the suppression is due to a modification of the k_T dependence of the lead TMD, comparing to the proton TMD. In the latter case, the suppression is much stronger and is mainly due to the suppression of the maximum of the dipole lead TMD, comparing to the proton TMD at small x. The observed trends align with predictions based on gluon saturation. Our study further highlights the potential of future forward detectors at LHC. In particular, the FoCal calorimeter, with its very forward pseudorapidity coverage, probes the nuclear target at significantly smaller values of x, making it particularly sensitive to the potential gluon saturation signals.

Acknowledgments

We thank I. Grabowska-Bold for discussions. The work was suported by the Polish National Science Centre, grant no. 2020/39/O/ST2/03011.

References

- [1] L3 collaboration, O. Adrian et al., Determination of alpha-s from hadronic event shapes measured on the Z0 resonance, Phys. Lett. B 284 (1992) 471–481.
- [2] ALEPH Collaboration, Measurement of α_s from the structure of particle clusters produced in hadronic z decays, Physics Letters B 257 (1991) 479-491.
- [3] A. Banfi, G. P. Salam and G. Zanderighi, *Phenomenology of event shapes at hadron colliders*, *JHEP* **06** (2010) 038, [1001.4082].
- [4] A. Gehrmann-De Ridder, T. Gehrmann, E.W.N. Glover and G. Heinrich, NNLO corrections to event shapes in e⁺e⁻ annihilation, Journal of High Energy Physics **2007** (dec, 2007) 094.
- [5] S. Weinzierl, Next-to-next-to-leading order corrections to three-jet observables in electron-positron annihilation, Physical Review Letters 101 (Oct., 2008).
- [6] S. Weinzierl, Event shapes and jet rates in electron-positron annihilation at nnlo, Journal of High Energy Physics 2009 (June, 2009) 041-041.
- [7] T. Becher and M. D. Schwartz, A precise determination of αs from lep thrust data using effective field theory, Journal of High Energy Physics 2008 (July, 2008) 034–034.
- [8] R. Abbate, M. Fickinger, A. H. Hoang, V. Mateu and I. W. Stewart, Thrust at N³LL with power corrections and a precision global fit for $\alpha_s(m_z)$, Physical Review D 83 (apr. 2011).
- [9] Y.-t. Chien and M. D. Schwartz, Resummation of heavy jet mass and comparison to lep data, Journal of High Energy Physics **2010** (Aug., 2010).
- [10] C. L. Basham, L. S. Brown, S. D. Ellis and S. T. Love, Energy Correlations in electron -Positron Annihilation: Testing QCD, Phys. Rev. Lett. 41 (1978) 1585.
- [11] C. L. Basham, L. S. Brown, S. D. Ellis and S. T. Love, Energy Correlations in electron-Positron Annihilation in Quantum Chromodynamics: Asymptotically Free Perturbation Theory, Phys. Rev. D 19 (1979) 2018.
- [12] OPAL Collaboration, An improved measuremetts of $\alpha_s(m_{Z^0})$ using energy correlations with the opal detector at lep, Physics Letters B **276** (1992) 547–564.
- [13] JADE Collaboration, Measurement of energy-energy correlations in $e^+e^- \rightarrow hadrons$ at \sqrt{s} =29 gev, Phys. Rev. D **31** (Jun, 1985) 2724–2731.
- [14] OPAL Collaboration, A measurement of energy correlations and a determination of $\alpha_s(m_{Z^0}^2)$ in e^+e^- annihilations at $\sqrt{s}=91$ GeV, Physics Letters B **252** (1990) 159–169.

- [15] D. Neill, G. Vita, I. Vitev and H. X. Zhu, Energy-Energy Correlators for Precision QCD, in Snowmass 2021, 3, 2022. 2203.07113.
- [16] I. Moult and H. X. Zhu, Energy Correlators: A Journey From Theory to Experiment, 2506.09119.
- [17] L. J. Dixon, M.-X. Luo, V. Shtabovenko, T.-Z. Yang and H. X. Zhu, Analytical Computation of Energy-Energy Correlation at Next-to-Leading Order in QCD, Phys. Rev. Lett. 120 (2018) 102001, [1801.03219].
- [18] D. M. Hofman and J. Maldacena, Conformal collider physics: Energy and charge correlations, JHEP 05 (2008) 012, [0803.1467].
- [19] A. Ali, E. Pietarinen and W. Stirling, Transverse energy-energy correlations: A test of perturbative qcd for the proton-antiproton collider, Physics Letters B 141 (1984) 447–454.
- [20] H. Li, I. Vitev and Y. Zhu, Transverse-energy-energy correlations in deep inelastic scattering, Journal of High Energy Physics **2020** (11, 2020).
- [21] ATLAS Collaboration, Measurement of transverse energy-energy correlations in multi-jet events in pp collisions at $\sqrt{s} = 7$ tev using the atlas detector and determination of the strong coupling constant $\alpha_s(m_z)$, Physics Letters B **750** (Nov., 2015) 427-447.
- [22] ATLAS Collaboration, Determination of the strong coupling constant from transverse energy-energy correlations in multijet events at $\sqrt{s}=13$ TeV with the ATLAS detector, JHEP **2023** (July, 2023).
- [23] D. d'Enterria et al., Physics with high-luminosity proton-nucleus collisions at the LHC, 2504.04268.
- [24] L. Gribov, E. Levin and M. Ryskin, Semihard processes in qcd, Physics Reports 100 (1983) 1–150.
- [25] A. H. Mueller and J.-w. Qiu, Gluon Recombination and Shadowing at Small Values of x, Nucl. Phys. B **268** (1986) 427–452.
- [26] Y. V. Kovchegov and E. Levin, Quantum chromodynamics at high energy, vol. 33. Cambridge University Press, 8, 2012, 10.1017/CBO9781139022187.
- [27] F. Gelis, E. Iancu, J. Jalilian-Marian and R. Venugopalan, The Color Glass Condensate, Ann. Rev. Nucl. Part. Sci. 60 (2010) 463–489, [1002.0333].
- [28] BRAHMS collaboration, I. Arsene et al., On the evolution of the nuclear modification factors with rapidity and centrality in d + Au collisions at s(NN)**(1/2) = 200-GeV, Phys. Rev. Lett. 93 (2004) 242303, [nucl-ex/0403005].
- [29] F. D. Aaron, H. Abramowicz and et. al., Combined measurement and qcd analysis of the inclusive e ± p scattering cross sections at hera, Journal of High Energy Physics 2010 (Jan., 2010).
- [30] STAR collaboration, M. S. Abdallah and et. al., Evidence for nonlinear gluon effects in qcd and their mass number dependence at star, Phys. Rev. Lett. 129 (Aug, 2022) 092501.
- [31] L. Frankfurt, V. Guzey and M. Strikman, Leading Twist Nuclear Shadowing Phenomena in Hard Processes with Nuclei, Phys. Rept. 512 (2012) 255–393, [1106.2091].
- [32] A. H. Rezaeian, Semi-inclusive photon-hadron production in pp and pA collisions at RHIC and LHC, Phys. Rev. D 86 (2012) 094016, [1209.0478].
- [33] J. Jalilian-Marian and A. H. Rezaeian, Prompt photon production and photon-hadron correlations at RHIC and the LHC from the Color Glass Condensate, Phys. Rev. D 86 (2012) 034016, [1204.1319].

- [34] B. Ducloué, T. Lappi and H. Mäntysaari, Isolated photon production in proton-nucleus collisions at forward rapidity, Phys. Rev. D 97 (2018) 054023, [1710.02206].
- [35] V. P. Goncalves, Y. Lima, R. Pasechnik and M. Šumbera, Isolated photon production and pion-photon correlations in high-energy pp and pA collisions, Phys. Rev. D 101 (2020) 094019, [2003.02555].
- [36] G. Sampaio dos Santos, G. Gil da Silveira and M. V. T. Machado, Prompt photon production in high-energy pA collisions at forward rapidity, Phys. Rev. C 102 (2020) 054901, [2006.15743].
- [37] K. Golec-Biernat, L. Motyka and T. Stebel, Prompt photon production in proton collisions as a probe of parton scattering in high energy limit, Phys. Rev. D 103 (2021) 034013, [2010.00468].
- [38] G. S. d. Santos, G. G. da Silveira and M. V. T. Machado, A study on the isolated photon production in nuclear collisions at the CERN-LHC energies, J. Phys. G 49 (2022) 045005, [2011.08154].
- [39] S. Benić, O. Garcia-Montero and A. Perkov, Isolated photon-hadron production in high energy pp and pA collisions at RHIC and LHC, Phys. Rev. D 105 (2022) 114052, [2203.01685].
- [40] Y. N. Lima, A. V. Giannini and V. P. Goncalves, Isolated photon production in pp collisions at forward rapidities and high multiplicity events, Eur. Phys. J. A 60 (2024) 54, [2302.13720].
- [41] I. Ganguli, A. van Hameren, P. Kotko and K. Kutak, Forward γ+jet production in proton-proton and proton-lead collisions at LHC within the FoCal calorimeter acceptance, Eur. Phys. J. C 83 (2023) 868, [2306.04706].
- [42] S. P. Adhya, K. Kutak, W. Placzek, M. Rohrmoser and K. Tywoniuk, Predictions for photon-jet correlations at forward rapidities in heavy-ion collisions, Eur. Phys. J. C 85 (2025) 343, [2409.06675].
- [43] K. Roy and R. Venugopalan, NLO impact factor for inclusive photon+dijet production in e + A DIS at small x, Phys. Rev. D 101 (2020) 034028, [1911.04530].
- [44] K. Roy and R. Venugopalan, Inclusive prompt photon production in electron-nucleus scattering at small x, JHEP 05 (2018) 013, [1802.09550].
- [45] I. Kolbé, K. Roy, F. Salazar, B. Schenke and R. Venugopalan, Inclusive prompt photon-jet correlations as a probe of gluon saturation in electron-nucleus scattering at small x, JHEP 01 (2021) 052, [2008.04372].
- [46] ALICE collaboration, ALICE Collaboration, Letter of Intent: A Forward Calorimeter (FoCal) in the ALICE experiment, .
- [47] ATLAS collaboration, O. Solovyanov, ATLAS upgrades for High Luminosity LHC, PoS DIS2024 (2025) 278.
- [48] I. Ganguli, A. van Hameren, P. Kotko and K. Kutak, Forward γ +jet production in proton-proton and proton-lead collisions at lhc within the focal calorimeter acceptance, 2023.
- [49] Z.-B. Kang, R. Kao, M. Li and J. Penttala, Transverse Energy-Energy Correlators at Small x for Photon-Hadron Production, 2504.00069.
- [50] A. Gao, H. T. Li, I. Moult and H. X. Zhu, The transverse energy-energy correlator at next-to-next-to-leading logarithm, 2312.16408.
- [51] R. Engel, Photoproduction within the two component dual parton model. 1. Amplitudes and cross-sections, Z. Phys. C 66 (1995) 203–214.

- [52] S. Roesler, R. Engel and J. Ranft, The Monte Carlo event generator DPMJET-III, in International Conference on Advanced Monte Carlo for Radiation Physics, Particle Transport Simulation and Applications (MC 2000), pp. 1033-1038, 12, 2000. hep-ph/0012252. DOI.
- [53] K. Werner, F.-M. Liu and T. Pierog, Parton ladder splitting and the rapidity dependence of transverse momentum spectra in deuteron-gold collisions at RHIC, Phys. Rev. C 74 (2006) 044902, [hep-ph/0506232].
- [54] K. Werner, Revealing a deep connection between factorization and saturation: New insight into modeling high-energy proton-proton and nucleus-nucleus scattering in the EPOS4 framework, Phys. Rev. C 108 (2023) 064903, [2301.12517].
- [55] R. S. Fletcher, T. K. Gaisser, P. Lipari and T. Stanev, SIBYLL: An Event generator for simulation of high-energy cosmic ray cascades, Phys. Rev. D 50 (1994) 5710-5731.
- [56] E.-J. Ahn, R. Engel, T. K. Gaisser, P. Lipari and T. Stanev, Cosmic ray interaction event generator SIBYLL 2.1, Phys. Rev. D 80 (2009) 094003, [0906.4113].
- [57] N. N. Kalmykov, S. S. Ostapchenko and A. I. Pavlov, Quark-Gluon String Model and EAS Simulation Problems at Ultra-High Energies, Nucl. Phys. B Proc. Suppl. 52 (1997) 17–28.
- [58] S. Ostapchenko, Monte Carlo treatment of hadronic interactions in enhanced Pomeron scheme: I. QGSJET-II model, Phys. Rev. D 83 (2011) 014018, [1010.1869].
- [59] A. van Hameren, Katie: for parton-level event generation with k_t -dependent initial states, 1611.00680.
- [60] I. Balitsky, Operator expansion for high-energy scattering, Nucl. Phys. B 463 (1996) 99–160, [hep-ph/9509348].
- [61] Y. V. Kovchegov, Small x F(2) structure function of a nucleus including multiple pomeron exchanges, Phys. Rev. D 60 (1999) 034008, [hep-ph/9901281].
- [62] J. Jalilian-Marian, A. Kovner, A. Leonidov and H. Weigert, The BFKL equation from the Wilson renormalization group, Nucl. Phys. B 504 (1997) 415-431, [hep-ph/9701284].
- [63] A. Kovner, J. G. Milhano and H. Weigert, Relating different approaches to nonlinear QCD evolution at finite gluon density, Phys. Rev. D62 (2000) 114005, [hep-ph/0004014].
- [64] A. Kovner and J. G. Milhano, Vector potential versus color charge density in low x evolution, Phys. Rev. D61 (2000) 014012, [hep-ph/9904420].
- [65] H. Weigert, Unitarity at small Bjorken x, Nucl. Phys. A703 (2002) 823–860, [hep-ph/0004044].
- [66] E. Iancu, A. Leonidov and L. D. McLerran, Nonlinear gluon evolution in the color glass condensate. 1., Nucl. Phys. A692 (2001) 583-645, [hep-ph/0011241].
- [67] E. Ferreiro, E. Iancu, A. Leonidov and L. McLerran, Nonlinear gluon evolution in the color glass condensate. 2., Nucl. Phys. A 703 (2002) 489–538, [hep-ph/0109115].
- [68] S. Baranov, A. Bermudez Martinez and et. al., Cascade3 a monte carlo event generator based on tmds, The European Physical Journal C 81 (May, 2021).
- [69] M. Bury, A. van Hameren, H. Jung, K. Kutak, S. Sapeta and M. Serino, Calculations with off-shell matrix elements, TMD parton densities and TMD parton showers, Eur. Phys. J. C 78 (2018) 137, [1712.05932].
- [70] M. Bury, H. Van Haevermaet, A. Van Hameren, P. Van Mechelen, K. Kutak and M. Serino, Single inclusive jet production and the nuclear modification ratio at very forward rapidity in proton-lead collisions with $\sqrt{s_{NN}} = 5.02$ TeV, Phys. Lett. B 780 (2018) 185–190, [1712.08105].

- [71] H. Van Haevermaet, A. Van Hameren, P. Kotko, K. Kutak and P. Van Mechelen, *Trijets in k_{\rm T}-factorisation: matrix elements vs parton shower*, *Eur. Phys. J. C* **80** (2020) 610, [2004.07551].
- [72] ALICE collaboration, S. Acharya et al., Measurement of isolated photon-hadron correlations in $\sqrt{s_{\rm NN}} = 5.02$ TeV pp and p-Pb collisions, Phys. Rev. C 102 (2020) 044908, [2005.14637].
- [73] ALICE collaboration, S. Acharya et al., Measurement of isolated prompt photon production in pp and p-Pb collisions at the LHC, 2502.18054.
- [74] ATLAS collaboration, G. Aad et al., Measurement of the production cross section of an isolated photon associated with jets in proton-proton collisions at $\sqrt{s} = 7$ TeV with the ATLAS detector, Phys. Rev. D 85 (2012) 092014, [1203.3161].
- [75] ATLAS collaboration, M. Aaboud et al., Measurement of the cross section for isolated-photon plus jet production in pp collisions at $\sqrt{s} = 13$ TeV using the ATLAS detector, Phys. Lett. B 780 (2018) 578–602, [1801.00112].
- [76] S. Catani, M. Ciafaloni and F. Hautmann, *High-energy factorization and small x heavy flavor production*, *Nucl. Phys. B* **366** (1991) 135–188.
- [77] J. C. Collins and R. Ellis, Heavy quark production in very high-energy hadron collisions, Nucl. Phys. B **360** (1991) 3–30.
- [78] A. Dumitru, A. Hayashigaki and J. Jalilian-Marian, The Color glass condensate and hadron production in the forward region, Nucl. Phys. A 765 (2006) 464–482, [hep-ph/0506308].
- [79] M. Deak, F. Hautmann, H. Jung and K. Kutak, Forward Jet Production at the Large Hadron Collider, JHEP 09 (2009) 121, [0908.0538].
- [80] F. Dominguez, C. Marquet, B.-W. Xiao and F. Yuan, Universality of Unintegrated Gluon Distributions at small x, Phys. Rev. D 83 (2011) 105005, [1101.0715].
- [81] A. van Hameren, P. Kotko and K. Kutak, Multi-gluon helicity amplitudes with one off-shell leg within high energy factorization, JHEP 12 (2012) 029, [1207.3332].
- [82] A. van Hameren, P. Kotko and K. Kutak, Helicity amplitudes for high-energy scattering, JHEP 01 (2013) 078, [1211.0961].
- [83] A. Buckley, J. Ferrando, S. Lloyd, K. Nordström, B. Page, M. Rüfenacht et al., LHAPDF6: parton density access in the LHC precision era, Eur. Phys. J. C 75 (2015) 132, [1412.7420].
- [84] K. Kutak and S. Sapeta, Gluon saturation in dijet production in imml:math xmlns:mml="http://www.w3.org/1998/math/mathml" display="inline" jmml:mijp/mml:mijp/mml:mathj-pb collisions at the large hadron collider, Physical Review D 86 (Nov., 2012).
- [85] J. Kwiecinski, A. D. Martin and A. Stasto, A Unified BFKL and GLAP description of F2 data, Phys. Rev. D 56 (1997) 3991–4006, [hep-ph/9703445].
- [86] K. Kutak and J. Kwiecinski, Screening effects in the ultrahigh-energy neutrino interactions, Eur. Phys. J. C 29 (2003) 521, [hep-ph/0303209].